

## Trajectory tracking control of a quadrotor UAV based on sliding mode active disturbance rejection control\*

Yong Zhang<sup>a</sup>, Zengqiang Chen<sup>a,1</sup>, Mingwei Sun<sup>a</sup>, Xinghui Zhang<sup>b</sup>

<sup>a</sup>College of Artificial Intelligence, Nankai University,  
Tianjin, 300350, China  
chenzq@nankai.edu.cn

<sup>b</sup>Tianjin Sino-German University of Applied Sciences,  
Tianjin, 300350, China  
zhangdayong810@163.com

**Received:** June 11, 2018 / **Revised:** December 25, 2018 / **Published online:** June 27, 2019

**Abstract.** This paper proposes a sliding mode active disturbance rejection control scheme to deal with trajectory tracking control problems for the quadrotor unmanned aerial vehicle (UAV). Firstly, the differential signal of the reference trajectory can be obtained directly by using the tracking differentiator (TD), then the design processes of the controller can be simplified. Secondly, the estimated values of the UAV's velocities, angular velocities, total disturbance can be acquired by using extended state observer (ESO), and the total disturbance of the system can be compensated in the controller in real time, then the robustness and anti-interference capability of the system can be improved. Finally, the sliding mode controller based on TD and ESO is designed, the stability of the closed-loop system is proved by Lyapunov method. Simulation results show that the control scheme proposed in this paper can make the quadrotor track the desired trajectory quickly and accurately.

**Keywords:** sliding mode control, active disturbance rejection control (ADRC), extended state observer (ESO), quadrotor UAV, trajectory tracking control.

### 1 Introduction

Quadrotor UAV is an underactuated system, which has some advantages such as vertical takeoff and landing, autonomous hovering, high energy efficiency [13], autonomous control, etc. Quadrotor is widely used in civil and military fields. In the civil field, quadrotor UAV can be used in power inspection, ground monitoring, aerial photography, pesticide spraying. In the military field, because of its high covertness and reliability, it is very suitable for performing battlefield reconnaissance and assessment, target discovery and other military tasks [16]. However, the multivariable, nonlinear, strong coupling and sensitivity to disturbances of the quadrotor UAV system itself make it difficult to control [27].

\*This research was supported by the National Natural Science Foundation of China under grant No. 61573197, 61573199.

<sup>1</sup>Corresponding author.

Air resistance and other external disturbances are also encountered during the flight, so various external interference issues need to be considered when designing the controller. In addition, the dynamic model of the quadrotor UAV is complicated, and some of these aerodynamic parameters are difficult to measure accurately, thus these unknown uncertainties further increase the difficulty of designing the controller for quadrotor UAV. In consequence, trajectory tracking control [11,29] of quadrotor UAV has attracted attentions of the researchers widely.

At present, researchers have done a lot of algorithms for quadrotor UAV, these control algorithms can be divided into linear control algorithms, nonlinear control algorithms and intelligent control algorithms. In [18,28], PID controller is proposed for controlling the quadrotor. In [23], LQR gain adjustment control is used to realize attitude and path tracking control for quadrotor UAV. Backstepping and sliding mode control have been used in quadrotor UAV, which presented in [5, 10, 19, 22]. In [20], robust control scheme is proposed to cope with the trajectory tracking problem for UAV. There are some other control methods for quadrotor UAV such as adaptive control [3, 6], predictive control [1], neural network control [8], fault tolerance control [4], etc. But these methods either rely on precise mathematical models or require knowledge of the upper bounds of uncertainties, which are easily influenced by internal uncertainties and unknown disturbances. In [25], an adaptive neural output-feedback controller have been established for a class of uncertain nonlinear systems with unmodeled dynamics and the lack of full-state measurements. In [30], adaptive fuzzy control scheme have been used for uncertain nonsmooth nonlinear systems. In [26], Robust fuzzy adaptive control strategy is used for a class of nonaffine stochastic nonlinear switched systems. Despite the adaptive neural control or adaptive fuzzy control, the control design process is complicated, programming is difficult, for multivariable and fast response system, is not very suitable. The control method proposed in this paper has fast tracking speed and strong anti-disturbance ability, the control design process is more simplified, the controller has fewer control parameters, this method is more suitable for engineering applications.

Active disturbance rejection control technique [12, 14, 15] is a new control strategy emerged in the 80s of last century. The ESO is the core of the whole system, which can estimate the total disturbance including internal unknown and external disturbances, and the total disturbance can be compensated by the state error feedback control law. ADRC is a control method that does not depend on accurate system model, it has fast tracking speed, high control precision and strong anti-disturbance ability, it has been widely used in many theoretical researches, experiments and engineering applications. Because the quadrotor UAV is continually affected by external disturbances and model uncertainties, this can destabilize the UAV easily. A better method to handle with these disturbances is ADRC strategy.

In this paper, a sliding mode active disturbance rejection control strategy is proposed to deal with some difficult control problems in the quadrotor unmanned aerial vehicle system such as nonlinearity, strong coupling and sensitive to disturbance. This control method neither depend on precise mathematical models nor require knowledge of the upper bounds of uncertainties, it not only can solve the difficulty of flight control, but also can eliminate the complicated external interference and get good flight performance.

The main idea is to combine the advantages of sliding mode control method to track the desired trajectory smoothly with the ability of ADRC to reject the model uncertainties and external disturbances. TD is used to obtain the differential signal of the reference trajectory, which can simplify the design processes of the controller. ESO is used to obtain the estimated values of the vehicles velocities, angular velocities, total disturbance, and the total disturbance of the system can be compensated in the controller. Finally, the sliding mode controller based on ADRC is designed, and the stability of the closed-loop system is analyzed by Lyapunov method.

This paper is organized as follows: A typical quadrotor mathematical model is introduced in Section 2. Sliding mode control scheme based on ADRC for quadrotor system is designed in Section 3. Stability of the quadrotor UAV system is proved in Section 4. Results of simulation experiment are illustrated in Section 5. Finally, some concluding remarks are given in Section 6.

## 2 System modelling

The scheme of the quadrotor UAV [7, 17, 21] is shown in Fig. 1. In this figure,  $F_i$  ( $i = 1, 2, 3, 4$ ) are lift forces of the four rotors, respectively.  $O_b = \{X_b, Y_b, Z_b\}$  is the body fixed frame,  $O_e = \{X_e, Y_e, Z_e\}$  is the fixed frame with respect to the earth. Quadrotor UAV is an underactuated system with six degrees of freedom and only four control inputs, and it is also a system with some characteristics such as multivariate, strong coupling, nonlinearity, sensitive to disturbance.

Assume that the quadrotor UAV is a rigid body and the body structure is symmetrical. The mathematical model of the quadrotor UAV system [2, 24] can be expressed by the following equations:

$$\begin{cases} \ddot{x} = \frac{1}{m}(F_x - k_f \dot{x}), \\ \ddot{y} = \frac{1}{m}(F_y - k_f \dot{y}), \\ \ddot{z} = \frac{1}{m}(F_z - mg - k_f \dot{z}), \\ \ddot{\theta} = \frac{l(-F_1 + F_2 + F_3 - F_4 - k_f \dot{\theta})}{I_y} + \frac{(I_z - I_x)}{I_y} \dot{\phi} \dot{\psi}, \\ \ddot{\phi} = \frac{l(-F_1 - F_2 + F_3 + F_4 - k_f \dot{\phi})}{I_x} + \frac{(I_y - I_z)}{I_x} \dot{\theta} \dot{\psi}, \\ \ddot{\psi} = \frac{k_c(-F_1 + F_2 - F_3 + F_4) - k_f \dot{\psi}}{I_z} + \frac{(I_x - I_y)}{I_z} \dot{\theta} \dot{\phi}, \end{cases} \quad (1)$$

where

$$\begin{bmatrix} F_x \\ F_y \\ F_z \end{bmatrix} = (F_1 + F_2 + F_3 + F_4) \begin{bmatrix} \cos \psi \sin \theta \cos \phi + \sin \psi \sin \phi \\ \sin \psi \sin \theta \cos \phi - \sin \phi \cos \psi \\ \cos \theta \cos \phi \end{bmatrix} \quad (2)$$

$x, y, z$  are positions of the quadrotor,  $\theta$  is the pitch angle,  $\phi$  is the roll angle, and  $\psi$  is the yaw angle.  $F_1, F_2, F_3, F_4$  are lift forces of the four rotors respectively, and other system parameters are shown in Table 1.

In order to simplify the design procedures and the presentation of the quadrotor flight system, the virtual control variables of the whole system  $U_1, U_2, U_3, U_4$  are introduced

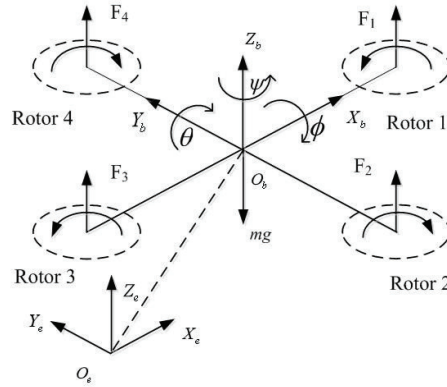


Figure 1. Free-body diagram of quadrotor.

Table 1. Quadrotor system parameters.

$m$	Quality of the quadrotor	2	kg
$l$	Length between the centre of the aircraft and the rotor	0.35	m
$k_c$	Torque coefficient	0.035	m
$k_f$	Coefficient of air resistance	0.012	$\text{N s}^2/\text{rad}^2$
$I_x$	Rotational inertia of the $x$ -axis	1.25	$\text{Kg m}^2$
$I_y$	Rotational inertia of the $y$ -axis	1.25	$\text{Kg m}^2$
$I_z$	Rotational inertia of the $z$ -axis	2.5	$\text{Kg m}^2$
$g$	Gravitational acceleration	9.8	$\text{m/s}^2$

to transform with the lift forces  $F_1, F_2, F_3, F_4$ . The variable transformation formula can be expressed as follows:

$$\begin{bmatrix} U_1 \\ U_2 \\ U_3 \\ U_4 \end{bmatrix} = \begin{bmatrix} 1/m & 1/m & 1/m & 1/m \\ -l/I_y & l/I_y & l/I_y & -l/I_y \\ -l/I_x & -l/I_x & l/I_x & l/I_x \\ -k_c/I_z & k_c/I_z & -k_c/I_z & k_c/I_z \end{bmatrix} \begin{bmatrix} F_1 \\ F_2 \\ F_3 \\ F_4 \end{bmatrix}. \tag{3}$$

Combining (1), (2) and (3), the mathematical model of the quadrotor can be rewritten as

$$\begin{cases} \ddot{x} = U_1(\cos \psi \sin \theta \cos \phi + \sin \psi \sin \phi) - \frac{1}{m} k_f \dot{x}, \\ \ddot{y} = U_1(\sin \psi \sin \theta \cos \phi - \cos \psi \sin \phi) - \frac{1}{m} k_f \dot{y}, \\ \ddot{z} = U_1(\cos \phi \cos \theta) - g - \frac{1}{m} k_f \dot{z}, \\ \ddot{\theta} = U_2 - \frac{l k_f}{I_y} \dot{\theta} + \frac{I_z - I_x}{I_y} \dot{\phi} \dot{\psi}, \\ \ddot{\phi} = U_3 - \frac{l k_f}{I_x} \dot{\phi} + \frac{I_y - I_z}{I_x} \dot{\theta} \dot{\psi}, \\ \ddot{\psi} = U_4 - \frac{k_f}{I_z} \dot{\psi} + \frac{I_x - I_y}{I_z} \dot{\theta} \dot{\phi}. \end{cases}$$

Since the position loop has only one control input  $U_1$ , therefore, we can select two intermediate variables  $\theta$  and  $\phi$  from the attitude loop to control position loop indirectly.

Set

$$\begin{cases} U_x = U_1(\cos \psi \sin \theta \cos \phi + \sin \psi \sin \phi), \\ U_y = U_1(\sin \psi \sin \theta \cos \phi - \cos \psi \sin \phi), \\ U_z = U_1(\cos \phi \cos \theta). \end{cases} \quad (4)$$

Solving system (4), we get

$$U_1 = \frac{U_z}{\cos \phi \cos \theta}, \quad (5)$$

$$\theta = \arctan\left(\frac{U_x \cos \psi + U_y \sin \psi}{U_z}\right), \quad (6)$$

$$\phi = \arctan\left(\cos \theta \frac{U_x \sin \psi - U_y \cos \psi}{U_z}\right). \quad (7)$$

### 3 Control scheme

In consideration of the quadrotor dynamic characteristics, it is concluded that the quadrotor system has two loops, and the two loops can be divided into six channels. The altitude  $z$  channel and the yaw angle  $\psi$  channel are independent channels, the  $x - \theta$  channels and the  $y - \phi$  channels are two cascade subsystems.

Firstly, the sliding mode controller based on ADRC is applied in the position loop for translational movements. Using the reference trajectory  $x_d, y_d, z_d$ , the virtual inputs  $U_x, U_y, U_z$  can be obtained, then  $U_1, \theta_d, \phi_d$  will be calculated through equations (5), (6), (7), respectively. Then, the same control strategy is used in attitude loop,  $\theta_d, \phi_d, \psi_d$  are used in the rotational subsystem as the Euler angle references. Finally,  $U_2, U_3, U_4$  can be obtained to achieve the quadrotor UAV stabilization. The block diagram of the quadrotor UAV control scheme is depicted in Fig. 2.

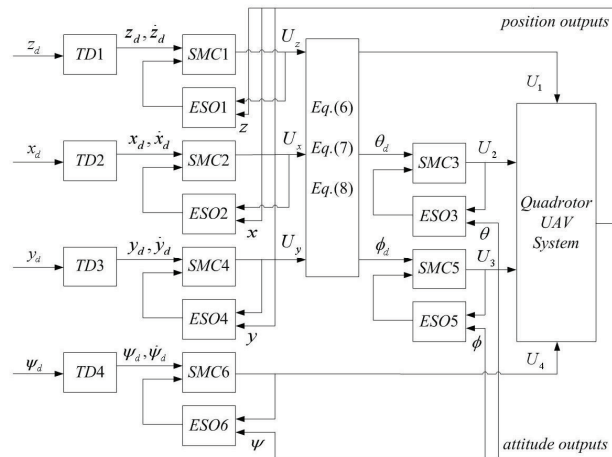


Figure 2. Control scheme.

### 3.1 Tracking differentiator design

Since the quadrotor is an underactuated system, which has four control objectives: altitude  $z$ , position  $x$ , position  $y$  and yaw angle  $\psi$ , therefore the TD [25] should be designed for these four channels. Taking the altitude channel as an example, the design algorithm is given by

$$\begin{cases} \dot{v}_{z1} = v_{z2}, \\ \dot{v}_{z2} = \text{fhan}(v_{z1} - z_d, v_{z2}, r, h). \end{cases}$$

Here  $v_{z1}$  is the tracking signal for  $z_d$ , and  $v_{z2}$  is the differential signal of  $v_{z1}$ ,  $r$  is the speed factor, which can determine the convergence speed, and  $h$  is the filtering factor,  $\text{fhan}(\cdot)$  denotes the optimal synthetic rapid control function, which is proposed as

$$\begin{cases} d = rh^2, & a_0 = hv_{z2}, & y = (v_{z1} - z_d) + a_0, \\ a_1 = \sqrt{d(d + 8|y|)}, & a_2 = a_0 + \text{sign } y \frac{a_1 - d}{2}, \\ a = (a_0 + y) \text{fsg}(y, d) + a_2(1 - \text{fsg}(y, d)), \\ \text{fsg}(x, d) = \frac{1}{2}(\text{sign}(x + d) - \text{sign}(x - d)), \\ \text{fhan} = -r\left(\frac{a}{d}\right) \text{fsg}(a, d) - r \text{sign } a(1 - \text{fsg}(a, d)). \end{cases}$$

### 3.2 Extended state observer design

In order to compensate the disturbances in the controller and to obtain the velocities and angular velocities of the UAV, let  $x_1 = x$ ,  $x_2 = \dot{x}$ ,  $x_3 = f_1$ ,  $y_1 = y$ ,  $y_2 = \dot{y}$ ,  $y_3 = f_2$ ,  $z_1 = z$ ,  $z_2 = \dot{z}$ ,  $z_3 = f_3$ ,  $\theta_1 = \theta$ ,  $\theta_2 = \dot{\theta}$ ,  $\theta_3 = f_4$ ,  $\phi_1 = \phi$ ,  $\phi_2 = \dot{\phi}$ ,  $\phi_3 = f_5$ ,  $\psi_1 = \psi$ ,  $\psi_2 = \dot{\psi}$ ,  $\psi_3 = f_6$ , where  $f_i$  ( $i = 1, 2, 3, 4, 5, 6$ ) are total disturbances of the each channel, therefore the six channels' ESO of the quadrotor UAV system can be designed as

$$\begin{cases} \dot{\hat{x}}_1 = \hat{x}_2 - \beta_1(\hat{x}_1 - x_1), & \dot{\hat{y}}_1 = \hat{y}_2 - \beta_1(\hat{y}_1 - y_1), \\ \dot{\hat{x}}_2 = \hat{x}_3 - \beta_2(\hat{x}_1 - x_1) + U_x, & \dot{\hat{y}}_2 = \hat{y}_3 - \beta_2(\hat{y}_1 - y_1) + U_y, \\ \dot{\hat{x}}_3 = -\beta_3(\hat{x}_1 - x_1), & \dot{\hat{y}}_3 = -\beta_3(\hat{y}_1 - y_1), \end{cases}$$

$$\begin{cases} \dot{\hat{z}}_1 = \hat{z}_2 - \beta_1(\hat{z}_1 - z_1), & \dot{\hat{\theta}}_1 = \hat{\theta}_2 - \beta_1(\hat{\theta}_1 - \theta_1), \\ \dot{\hat{z}}_2 = \hat{z}_3 - \beta_2(\hat{z}_1 - z_1) + U_z, & \dot{\hat{\theta}}_2 = \hat{\theta}_3 - \beta_2(\hat{\theta}_1 - \theta_1) + U_2, \\ \dot{\hat{z}}_3 = -\beta_3(\hat{z}_1 - z_1), & \dot{\hat{\theta}}_3 = -\beta_3(\hat{\theta}_1 - \theta_1), \end{cases}$$

$$\begin{cases} \dot{\hat{\phi}}_1 = \hat{\phi}_2 - \beta_1(\hat{\phi}_1 - \phi_1), & \dot{\hat{\psi}}_1 = \hat{\psi}_2 - \beta_1(\hat{\psi}_1 - \psi_1), \\ \dot{\hat{\phi}}_2 = \hat{\phi}_3 - \beta_2(\hat{\phi}_1 - \phi_1) + U_3, & \dot{\hat{\psi}}_2 = \hat{\psi}_3 - \beta_2(\hat{\psi}_1 - \psi_1) + U_4, \\ \dot{\hat{\phi}}_3 = -\beta_3(\hat{\phi}_1 - \phi_1), & \dot{\hat{\psi}}_3 = -\beta_3(\hat{\psi}_1 - \psi_1). \end{cases}$$

where  $\beta_1, \beta_2, \beta_3$  are observer gains, and  $\beta_1 = 3\omega_o$ ,  $\beta_2 = 3\omega_o^2$ ,  $\beta_3 = \omega_o^3$ ,  $\omega_o$  is the bandwidth of the ESO.

### 3.3 Sliding mode controller design

TD can provide the differential signals of the target track. The velocities, angular velocities and the total disturbance of the UAV are come from the ESO. Combining the advantages of the sliding mode control strategy to track the desired trajectory smoothly with the ability of the ADRC to handle with model uncertainties and external disturbances, therefore the sliding mode controller based on TD and ESO can be designed as follows.

The sliding mode function of the quadrotor's six channels can be written as

$$\begin{cases} s_x = k_{x2}e_x + \dot{e}_x, \\ s_y = k_{y2}e_y + \dot{e}_y, \\ s_z = k_{z2}e_z + \dot{e}_z, \end{cases} \quad \begin{cases} s_\theta = k_{\theta2}e_\theta + \dot{e}_\theta, \\ s_\phi = k_{\phi2}e_\phi + \dot{e}_\phi, \\ s_\psi = k_{\psi2}e_\psi + \dot{e}_\psi, \end{cases}$$

where  $k_{\theta2} > 0$ ,  $k_{\phi2} > 0$ ,  $k_{\psi2} > 0$ ,  $k_{x2} > 0$ ,  $k_{y2} > 0$ ,  $k_{z2} > 0$ , and

$$\begin{cases} e_x = x_1 - x_d, \\ e_y = y_1 - y_d, \\ e_z = z_1 - z_d, \end{cases} \quad \begin{cases} e_\theta = \theta_1 - \theta_d, \\ e_\phi = \phi_1 - \phi_d, \\ e_\psi = \psi_1 - \psi_d, \end{cases}$$

where  $x_d, y_d, z_d, \psi_d$  are references of the system,  $\theta_d, \phi_d$  are obtained from equations (6) and (7), respectively. Then the sliding mode control law based on ADRC of the six channels can be designed as

$$\begin{cases} U_x = -k_{x1}\hat{s}_x - \hat{v}_x - \hat{x}_3, \\ U_y = -k_{y1}\hat{s}_y - \hat{v}_y - \hat{y}_3, \\ U_z = -k_{z1}\hat{s}_z - \hat{v}_z - \hat{z}_3, \end{cases} \quad \begin{cases} U_2 = -k_{\theta1}\hat{s}_\theta - \hat{v}_\theta - \hat{\theta}_3, \\ U_3 = -k_{\phi1}\hat{s}_\phi - \hat{v}_\phi - \hat{\phi}_3, \\ U_4 = -k_{\psi1}\hat{s}_\psi - \hat{v}_\psi - \hat{\psi}_3, \end{cases} \quad (8)$$

where  $k_{\theta1} > 0$ ,  $k_{\phi1} > 0$ ,  $k_{\psi1} > 0$ ,  $k_{x1} > 0$ ,  $k_{y1} > 0$ ,  $k_{z1} > 0$ , and

$$\begin{cases} \hat{s}_x = k_{x2}\hat{e}_x + \dot{\hat{e}}_x, \\ \hat{s}_y = k_{y2}\hat{e}_y + \dot{\hat{e}}_y, \\ \hat{s}_z = k_{z2}\hat{e}_z + \dot{\hat{e}}_z, \end{cases} \quad \begin{cases} \hat{s}_\theta = k_{\theta2}\hat{e}_\theta + \dot{\hat{e}}_\theta, \\ \hat{s}_\phi = k_{\phi2}\hat{e}_\phi + \dot{\hat{e}}_\phi, \\ \hat{s}_\psi = k_{\psi2}\hat{e}_\psi + \dot{\hat{e}}_\psi, \end{cases}$$

$$\begin{cases} \hat{v}_x = k_{x2}\dot{\hat{e}}_x - \ddot{x}_d, \\ \hat{v}_y = k_{y2}\dot{\hat{e}}_y - \ddot{y}_d, \\ \hat{v}_z = k_{z2}\dot{\hat{e}}_z - \ddot{z}_d, \end{cases} \quad \begin{cases} \hat{v}_\theta = k_{\theta2}\dot{\hat{e}}_\theta - \ddot{\theta}_d, \\ \hat{v}_\phi = k_{\phi2}\dot{\hat{e}}_\phi - \ddot{\phi}_d, \\ \hat{v}_\psi = k_{\psi2}\dot{\hat{e}}_\psi - \ddot{\psi}_d, \end{cases}$$

$$\begin{cases} \hat{e}_x = \hat{x}_1 - x_d, \\ \hat{e}_y = \hat{y}_1 - y_d, \\ \hat{e}_z = \hat{z}_1 - z_d, \end{cases} \quad \begin{cases} \hat{e}_\theta = \hat{\theta}_1 - \theta_d, \\ \hat{e}_\phi = \hat{\phi}_1 - \phi_d, \\ \hat{e}_\psi = \hat{\psi}_1 - \psi_d, \end{cases}$$

$$\begin{cases} \dot{\hat{e}}_x = \hat{x}_2 - \dot{x}_d, \\ \dot{\hat{e}}_y = \hat{y}_2 - \dot{y}_d, \\ \dot{\hat{e}}_z = \hat{z}_2 - \dot{z}_d, \end{cases} \quad \begin{cases} \dot{\hat{e}}_\theta = \hat{\theta}_2 - \dot{\theta}_d, \\ \dot{\hat{e}}_\phi = \hat{\phi}_2 - \dot{\phi}_d, \\ \dot{\hat{e}}_\psi = \hat{\psi}_2 - \dot{\psi}_d, \end{cases}$$

and through equation (5), the control variable  $U_1$  can be obtained.

## 4 System stability analysis

### 4.1 Convergence of the ESO

Because the quadrotor system can be divided into six channels, and the mathematical model of the each channel can be written in a same state equation form, thereby, taking the position  $x$  channel as an example, its state space equation can be expressed as

$$\begin{cases} \dot{x}_1 = x_2, \\ \dot{x}_2 = x_3 + U_x, \\ \dot{x}_3 = \dot{f}, \end{cases} \quad (9)$$

where  $f$  is the total disturbance,  $U_x = U_1(\cos \psi \sin \theta \cos \phi + \sin \psi \sin \phi)$ , the linear extended state observer of equation (9) can be constructed as

$$\begin{cases} \dot{\hat{x}}_1 = \hat{x}_2 - \beta_1(\hat{x}_1 - x_1), \\ \dot{\hat{x}}_2 = \hat{x}_3 - \beta_2(\hat{x}_1 - x_1) + U_x, \\ \dot{\hat{x}}_3 = -\beta_3(\hat{x}_1 - x_1), \end{cases} \quad (10)$$

and  $L = [\beta_1 \ \beta_2 \ \beta_3]^T$  are observer gain parameters.

Let  $E_i(t) = x_i(t) - \hat{x}_i(t)$ ,  $i = 1, 2, 3$ , combining equations (9) and (10), the ESO estimation error dynamic equation can be written as

$$\begin{cases} \dot{E}_1 = -\beta_1 E_1 + E_2, \\ \dot{E}_2 = -\beta_2 E_1 + E_3, \\ \dot{E}_3 = -\beta_3 E_1 + \dot{f}. \end{cases} \quad (11)$$

Let  $\eta_i(t) = E_i(t)/\omega_o^{i-1}$ ,  $i = 1, 2, 3$ , then equation (11) can be rewritten as

$$\begin{cases} \dot{\eta}_1(t) = -\frac{\beta_1}{\omega_o^0} \eta_1 + \omega_o \eta_2, \\ \dot{\eta}_2(t) = -\frac{\beta_2}{\omega_o^1} \eta_1 + \omega_o \eta_3, \\ \dot{\eta}_3(t) = -\frac{\beta_3}{\omega_o^2} \eta_1 + \frac{\dot{f}}{\omega_o^2}. \end{cases} \quad (12)$$

Set  $\beta_1 = 3\omega_o$ ,  $\beta_2 = 3\omega_o^2$ ,  $\beta_3 = \omega_o^3$ , equation (12) can be expressed as

$$\dot{\eta}(t) = \omega_o M \eta(t) + N \frac{\dot{f}}{\omega_o^2}, \quad (13)$$

where

$$M = \begin{bmatrix} -3 & 1 & 0 \\ -3 & 0 & 1 \\ -3 & 0 & 0 \end{bmatrix}, \quad N = \begin{bmatrix} 0 \\ 0 \\ 1 \end{bmatrix}.$$

**Theorem 1.** Assuming that  $\dot{f}$  is bounded, then there exist a positive constant  $\varepsilon_i > 0$  and a finite time  $T > 0$  such that  $|E_i(t)| \leq \varepsilon_i$ ,  $i = 1, 2, 3$ , for all  $t \geq T > 0$ .

*Proof.* Solving (13), the following equation can be obtained:

$$\eta(t) = e^{\omega_o M t} \eta(0) + \int_0^t e^{\omega_o M (t-\tau)} N \frac{\dot{f}}{\omega_o^2} d\tau.$$

Let

$$Q(t) = \int_0^t e^{\omega_o M (t-\tau)} N \frac{\dot{f}}{\omega_o^2} d\tau.$$

Since  $\dot{f}$  is bounded,  $|\dot{f}| \leq D$ ,  $D > 0$ , then

$$|Q_i(t)| \leq \frac{D}{\omega_o^3} [|(M^{-1}N)_i| + |(M^{-1}e^{\omega_o M t}N)_i|]. \quad (14)$$

Since

$$M^{-1} = \begin{bmatrix} 0 & 0 & -1 \\ 1 & 0 & -3 \\ 0 & 1 & -3 \end{bmatrix},$$

then

$$|(M^{-1}N)_i| = \begin{cases} 1, & i = 1, \\ 3, & i = 2, 3. \end{cases} \quad (15)$$

Since  $M$  is a Hurwitz matrix, there exists a finite time  $T > 0$  such that for all  $t \geq T$ ,  $i, j = 1, 2, 3$ ,

$$\begin{cases} |(e^{\omega_o M t})_{ij}| \leq \frac{1}{\omega_o^3}, \\ |(e^{\omega_o M t}N)_i| \leq \frac{1}{\omega_o^3}. \end{cases}$$

Since  $T$  depends on  $\omega_o M$  [31], then set

$$M^{-1} = \begin{bmatrix} a_{11} & a_{12} & a_{13} \\ a_{21} & a_{22} & a_{23} \\ a_{31} & a_{32} & a_{33} \end{bmatrix}, \quad e^{\omega_o M t} = \begin{bmatrix} b_{11} & b_{12} & b_{13} \\ b_{21} & b_{22} & b_{23} \\ b_{31} & b_{32} & b_{33} \end{bmatrix}.$$

For all  $t \geq T$ ,

$$|(M^{-1}e^{\omega_o M t}N)_i| = |a_{i1}b_{13} + a_{i2}b_{23} + a_{i3}b_{33}| \leq \begin{cases} \frac{1}{\omega_o^3}, & i = 1, \\ \frac{4}{\omega_o^3}, & i = 2, 3. \end{cases} \quad (16)$$

Combining (14), (15), (16), we get

$$|Q_i(t)| \leq \frac{3D}{\omega_o^3} + \frac{4D}{\omega_o^6}. \quad (17)$$

Let  $\eta_s(0) = |\eta_1(0)| + |\eta_2(0)| + |\eta_3(0)|$  and for all  $t \geq T$ ,  $i = 1, 2, 3$ ,

$$|[e^{\omega_o M t}\eta(0)]_i| \leq \frac{\eta_s(0)}{\omega_o^3}, \quad (18)$$

then

$$|\eta_i(t)| \leq \frac{\eta_s(0)}{\omega_o^3} + \frac{3D}{\omega_o^3} + \frac{4D}{\omega_o^6}. \quad (19)$$

Let  $E_s(0) = \|E_1(0)\| + |E_2(0)| + |E_3(0)|$ , according to  $\eta_i(t) = E_i(t)/\omega_o^{i-1}$  and (17), (18), (19), then

$$|E_i(t)| \leq \frac{E_s(0)}{\omega_o^3} + \frac{3D}{\omega_o^{4-i}} + \frac{4D}{\omega_o^{7-i}} = \varepsilon_i. \quad (20)$$

From equation (20), if the total disturbance is bounded, then the estimation errors of the ESO are convergent, and when increasing the bandwidth  $\omega_o$  of the ESO,  $E_i(t)$  is going to zero.  $\square$

## 4.2 System stability analysis

**Assumption 1.** The state variables of the quadrotor UAV are measurable and can be used for the sliding mode controller design [9].

**Assumption 2.** Reference trajectory  $x_d, y_d, z_d, \psi_d$  are bounded.

**Theorem 2.** Assuming that  $f_i$  ( $i = 1, 2, 3, 4, 5, 6$ ) are bounded, then there exist constants  $k_{\theta i} > 0$  ( $i = 1, 2$ ),  $k_{\phi i} > 0$  ( $i = 1, 2$ ),  $k_{\psi i} > 0$  ( $i = 1, 2$ ),  $k_{x i} > 0$  ( $i = 1, 2$ ),  $k_{y i} > 0$  ( $i = 1, 2$ ),  $k_{z i} > 0$  ( $i = 1, 2$ ) such that the closed-loop system is stable.

*Proof.* Define the Lyapunov function of the quadrotor system as

$$V = \frac{1}{2}s_x^2 + \frac{1}{2}s_y^2 + \frac{1}{2}s_z^2 + \frac{1}{2}s_\theta^2 + \frac{1}{2}s_\phi^2 + \frac{1}{2}s_\psi^2,$$

then

$$\begin{aligned} \dot{V} &= s_x \dot{s}_x + s_y \dot{s}_y + s_z \dot{s}_z + s_\theta \dot{s}_\theta + s_\phi \dot{s}_\phi + s_\psi \dot{s}_\psi \\ &= s_x(k_{x2}\dot{e}_x + \ddot{e}_x) + s_y(k_{y2}\dot{e}_y + \ddot{e}_y) + s_z(k_{z2}\dot{e}_z + \ddot{e}_z) \\ &\quad + s_\theta(k_{\theta2}\dot{e}_\theta + \ddot{e}_\theta) + s_\phi(k_{\phi2}\dot{e}_\phi + \ddot{e}_\phi) + s_\psi(k_{\psi2}\dot{e}_\psi + \ddot{e}_\psi) \\ &= s_x(k_{x2}\dot{e}_x + U_x + f_1 - \ddot{x}_d) + s_y(k_{y2}\dot{e}_y + U_y + f_2 - \ddot{y}_d) \\ &\quad + s_z(k_{z2}\dot{e}_z + U_z + f_3 - \ddot{z}_d) + s_\theta(k_{\theta2}\dot{e}_\theta + U_2 + f_4 - \ddot{\theta}_d) \\ &\quad + s_\phi(k_{\phi2}\dot{e}_\phi + U_3 + f_5 - \ddot{\phi}_d) + s_\psi(k_{\psi2}\dot{e}_\psi + U_4 + f_6 - \ddot{\psi}_d). \end{aligned} \quad (21)$$

Combining (8), (21), we have

$$\begin{aligned} \dot{V} &= s_x(k_{x2}\dot{e}_x - k_{x1}\hat{s}_x - \hat{v}_x - \hat{x}_3 + x_3 - \ddot{x}_d) \\ &\quad + s_y(k_{y2}\dot{e}_y - k_{y1}\hat{s}_y - \hat{v}_y - \hat{y}_3 + y_3 - \ddot{y}_d) \\ &\quad + s_z(k_{z2}\dot{e}_z - k_{z1}\hat{s}_z - \hat{v}_z - \hat{z}_3 + z_3 - \ddot{z}_d) \\ &\quad + s_\theta(k_{\theta2}\dot{e}_\theta - k_{\theta1}\hat{s}_\theta - \hat{v}_\theta - \hat{\theta}_3 + \theta_3 - \ddot{\theta}_d) \\ &\quad + s_\phi(k_{\phi2}\dot{e}_\phi - k_{\phi1}\hat{s}_\phi - \hat{v}_\phi - \hat{\phi}_3 + \phi_3 - \ddot{\phi}_d) \\ &\quad + s_\psi(k_{\psi2}\dot{e}_\psi - k_{\psi1}\hat{s}_\psi - \hat{v}_\psi - \hat{\psi}_3 + \psi_3 - \ddot{\psi}_d) \\ &= s_x(k_{x2}\tilde{x}_2 + \tilde{x}_3 - k_{x1}\hat{s}_x) + s_y(k_{y2}\tilde{y}_2 + \tilde{y}_3 - k_{y1}\hat{s}_y) \\ &\quad + s_z(k_{z2}\tilde{z}_2 + \tilde{z}_3 - k_{z1}\hat{s}_z) + s_\theta(k_{\theta2}\tilde{\theta}_2 + \tilde{\theta}_3 - k_{\theta1}\hat{s}_\theta) \\ &\quad + s_\phi(k_{\phi2}\tilde{\phi}_2 + \tilde{\phi}_3 - k_{\phi1}\hat{s}_\phi) + s_\psi(k_{\psi2}\tilde{\psi}_2 + \tilde{\psi}_3 - k_{\psi1}\hat{s}_\psi) \end{aligned}$$

$$\begin{aligned}
&= -k_{x1}s_x^2 + s_x [k_{x1}k_{x2}\tilde{x}_1 + (k_{x1} + k_{x2})\tilde{x}_2 + \tilde{x}_3] \\
&\quad - k_{y1}s_y^2 + s_y [k_{y1}k_{y2}\tilde{y}_1 + (k_{y1} + k_{y2})\tilde{y}_2 + \tilde{y}_3] \\
&\quad - k_{z1}s_z^2 + s_z [k_{z1}k_{z2}\tilde{z}_1 + (k_{z1} + k_{z2})\tilde{z}_2 + \tilde{z}_3] \\
&\quad - k_{\theta 1}s_{\theta}^2 + s_{\theta} [k_{\theta 1}k_{\theta 2}\tilde{\theta}_1 + (k_{\theta 1} + k_{\theta 2})\tilde{\theta}_2 + \tilde{\theta}_3] \\
&\quad - k_{\phi 1}s_{\phi}^2 + s_{\phi} [k_{\phi 1}k_{\phi 2}\tilde{\phi}_1 + (k_{\phi 1} + k_{\phi 2})\tilde{\phi}_2 + \tilde{\phi}_3] \\
&\quad - k_{\psi 1}s_{\psi}^2 + s_{\psi} [k_{\psi 1}k_{\psi 2}\tilde{\psi}_1 + (k_{\psi 1} + k_{\psi 2})\tilde{\psi}_2 + \tilde{\psi}_3], \tag{22}
\end{aligned}$$

where  $\tilde{x}_i$  ( $i = 1, 2, 3$ ),  $\tilde{y}_i$  ( $i = 1, 2, 3$ ),  $\tilde{z}_i$  ( $i = 1, 2, 3$ ),  $\tilde{\theta}_i$  ( $i = 1, 2, 3$ ),  $\tilde{\phi}_i$  ( $i = 1, 2, 3$ ),  $\tilde{\psi}_i$  ( $i = 1, 2, 3$ ) are observed errors of the ESO. According to Theorem 1, since the ESO can make the errors converge to zero, therefore equation (22) can be rewritten as

$$\dot{V} \approx -k_{x1}s_x^2 - k_{y1}s_y^2 - k_{z1}s_z^2 - k_{\theta 1}s_{\theta}^2 - k_{\phi 1}s_{\phi}^2 - k_{\psi 1}s_{\psi}^2 \leq 0.$$

Therefore, if only  $k_{\theta i} > 0$  ( $i = 1, 2$ ),  $k_{\phi i} > 0$  ( $i = 1, 2$ ),  $k_{\psi i} > 0$  ( $i = 1, 2$ ),  $k_{x i} > 0$  ( $i = 1, 2$ ),  $k_{y i} > 0$  ( $i = 1, 2$ ),  $k_{z i} > 0$  ( $i = 1, 2$ ), then  $\dot{V} \leq 0$ , the closed-loop system of the quadrotor UAV is stable.  $\square$

## 5 Simulation results

The trajectory tracking simulation research of quadrotor UAV system is carried on using MATLAB. In order to illustrate the mobility and the validity of the proposed sliding mode ADRC strategy, a cylindrical spiral as a reference trajectory is used in the simulation, the effectiveness and advantages of the proposed control scheme are presented by comparative performances with the classical active disturbance rejection control.

The cylindrical spiral defined as:  $x_d = 0.5 \cos(0.5t)$  m,  $y_d = 0.5 \sin(0.5t)$  m,  $z_d = 2 + 0.1t$  m,  $\psi_d = 60^\circ$ . Set the initial position coordinates of the quadrotor UAV as  $[0, 0, 0]$ , while the initial attitude is  $[0, 0, 0]$ . Denoting  $\omega_1(t)$ ,  $\omega_2(t)$  and  $\omega_3(t)$  as system disturbances and adding them to the attitude loop, we can write

$$\begin{cases} \omega_1(t) = \text{sign}(\sin(0.9t)), \\ \omega_2(t) = \text{sign}(\sin(0.9t)) + \cos(0.3t), \\ \omega_3(t) = 0.5 \text{sign}(\sin(0.5t)) + \cos(0.3t) + 2 \cos(0.9t). \end{cases}$$

The parameters of the controller in the simulation are chosen as  $r = 2$ ,  $h = 0.01$ ,  $\omega_o = 50$ ,  $k_{x1} = 1$ ,  $k_{x2} = 1$ ,  $k_{y1} = 1$ ,  $k_{y2} = 4$ ,  $k_{z1} = 10$ ,  $k_{z2} = 50$ ,  $k_{\theta 1} = 0.1$ ,  $k_{\theta 2} = 0.1$ ,  $k_{\phi 1} = 0.1$ ,  $k_{\phi 2} = 20$ ,  $k_{\psi 1} = 10$ ,  $k_{\psi 2} = 30$ . The simulation results are shown in Figs. 3–7.

The results of trajectory tracking are demonstrated in Fig. 3. The simulation results of position control and attitude control are shown in Figs. 4 and 5, respectively. Figure 6 shows the error comparison of the two methods, and Fig. 7 shows the control inputs of the UAV system. In these figures, the black lines represent the reference trajectory, the blue

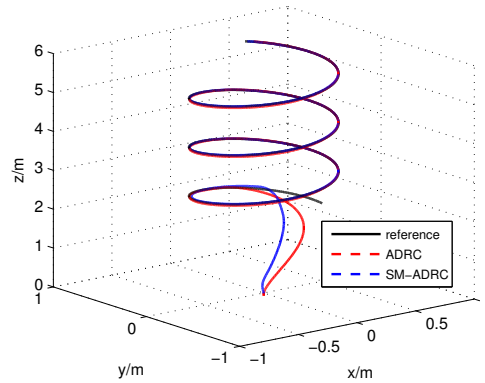


Figure 3. Trajectory tracking.

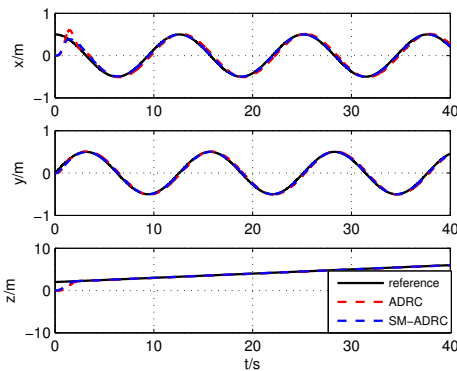


Figure 4. Position.

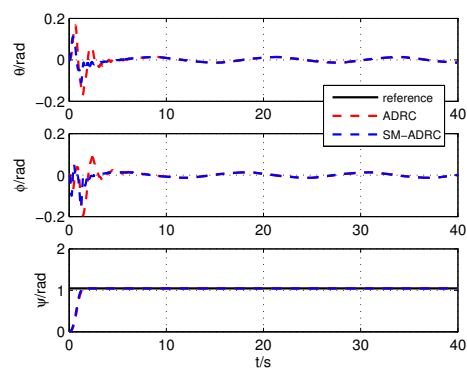


Figure 5. Attitude angle.

lines and the red lines represent the responses of the quadrotor UAV in cases of applying the sliding mode ADRC and classical ADRC, respectively.

It can be seen from the Fig. 3 that although the initial value of the position is far away from the reference trajectory, the control scheme that proposed in this paper can hold the quadrotor UAV track the cylindrical spiral trajectory instantly and accurately, and the performance of the sliding mode ADRC is better than the classical ADRC. The control strategy proposed in this paper has faster response, higher precision, less overshoot and less errors than classical ADRC. From Fig. 4, there is a higher overshoot in position  $x$  response controlled by classical ADRC than the response controlled by sliding mode ADRC, the response speed of the proposed method in position  $z$  is faster than the classical ADRC obviously and the tracking errors of the three positions achieved by the proposed controller are lesser than the errors that achieved by classical ADRC.

The ways that the sliding mode ADRC and the classical ADRC make the UAV follow the rotational references are shown in Fig. 5. Although the yaw angle responses of the two methods can track its corresponding desired trajectory rapidly and accurately, but

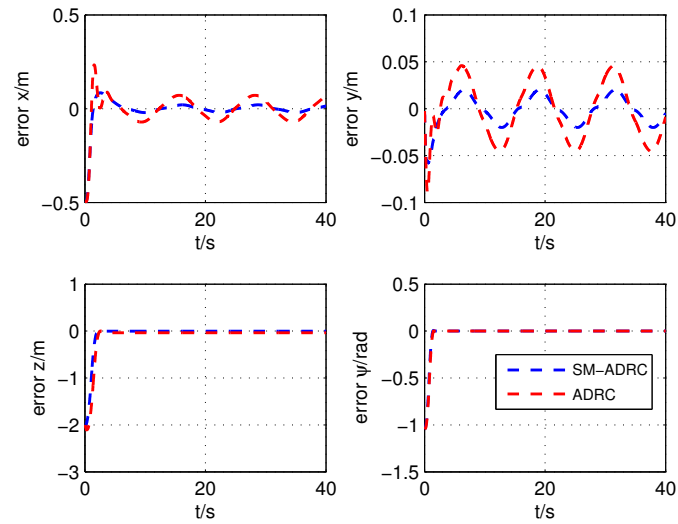


Figure 6. Errors.

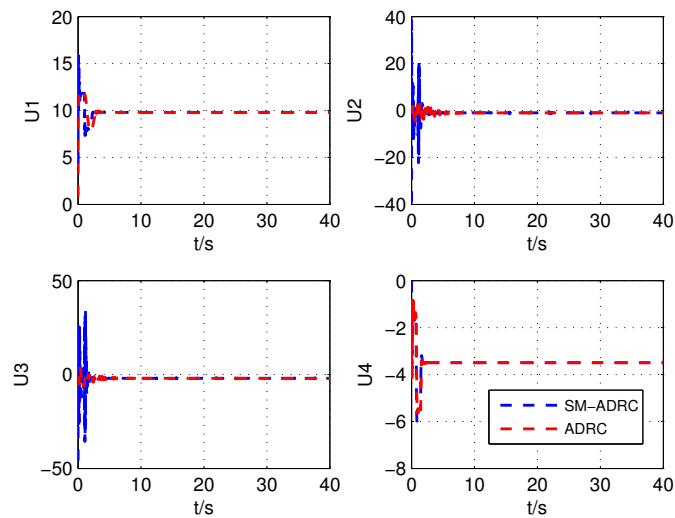


Figure 7. Control inputs.

the proposed scheme has better transient performances than classical ADRC, the pitch angle and the roll angle responses from the classical ADRC are more oscillatory at the beginning of the trajectory than the sliding mode ADRC. It can be clearly observed that the variation ranges of pitch angle and roll angle of sliding mode ADRC are more narrow and the adjustment time are shorter than classical ADRC.

It is clearly that the errors of the proposed scheme are less than classical ADRC, especially the error  $x$  and error  $y$  of classical method are much bigger than sliding mode

ADRC. From Fig. 6, it can be seen clearly that the performances are improved by sliding mode ADRC. Because there is no sign function in the controller, it can be seen from the Fig. 7 that the control inputs does not appear chattering in the sliding mode ADRC strategy.

## 6 Concluding remarks

The sliding mode ADRC scheme is designed for the quadrotor UAV in this paper. The differential signal of the reference trajectory can be obtained directly by using TD, the estimated values of the quadrotor's velocities, angular velocities, total disturbance can be acquired by ESO, and the total disturbance of the system can be compensated in the sliding mode controller.

Combining the sliding mode control and ADRC technique can maximize the advantages of the two control methods. Sliding mode control strategy can hold the quadrotor follow the reference trajectory in a smooth way with the ability of ADRC to reject the model uncertainties and external disturbances.

It can be seen from the simulation results that whether position tracking or angel tracking can follow the reference trajectory quickly and accurately. As can be seen from the comparison with classical ADRC, the performances of the quadrotor have been improved a lot. Therefore, it can be concluded that the control scheme proposed in this paper is an effective control method with strong robustness and anti-disturbance ability.

## References

1. K. Alexis, G. Nikolakopoulos, A. Tzes, Model predictive quadrotor control: Attitude, altitude and position experimental studies, *IET Control Theory Appl.*, **6**(12):1812–1827, 2012.
2. K. Alexis, G. Nikolakopoulos, A. Tzes, On trajectory tracking model predictive control of an unmanned quadrotor helicopter subject to aerodynamic disturbances, *Asian J. Control*, **16**(1): 209–224, 2014.
3. R. Amin, L. Aijun, M.U. Khan, S. Shamshirband, A. Kamsin, An adaptive trajectory tracking control of four rotor hover vehicle using extended normalized radial basis function network, *Mech. Syst. Signal Process.*, **83**(2017):53–74, 2017.
4. K. Buyukkabasakal, B. Fidan, A. Savran, Mixing adaptive fault tolerant control of quadrotor UAV, *Asian J. Control*, **19**(4):1441–1454, 2017.
5. F.Y. Chen, R.Q. Jiang, K.K. Zhang, B. Jiang, G. Tao, Robust backstepping sliding-mode control and observer-based fault estimation for a quadrotor UAV, *IEEE Trans. Ind. Electron.*, **63**(8):5044–5056, 2016.
6. F.Y. Chen, Q.B. Wu, B. Jiang, G. Tao, A reconfiguration scheme for quadrotor helicopter via simple adaptive control and quantum logic, *IEEE Trans. Ind. Electron.*, **62**(7):4328–4335, 2015.
7. P. Dey, S.R. Kurode, R. Ramachandran, Robust attitude control of quadrotor using sliding mode, in *Proceedings of the 2016 International Conference on Automatic Control and Dynamic Optimization Techniques, Pune, India, September 9–10, 2016*, IEEE, Piscataway, NJ, 2016, pp. 268–272.

8. T. Dierks, S. Jagannathan, Output feedback control of a quadrotor UAV using neural networks, *IEEE Trans. Neural Networks*, **21**(1):50–66, 2010.
9. X. Fang, J.K. Liu, Quadrotor UAV dynamic surface control, *Journal of Beijing University of Aeronautics and Astronautics*, **42**(8):1777–1784, 2016 (in Chinese).
10. N. Fethalla, M. Saad, H. Michalska, J. Ghommam, Robust observer-based backstepping controller for a quadrotor UAV, in *Proceedings of the 30th Canadian Conference on Electrical and Computer Engineering, Windsor, April 30–May 3, 2017*, IEEE, Piscataway, NJ, 2017, pp. 1–4.
11. C. Gao, Y.F. Jia, X.P. Liu, M. Chen, Modeling and prescribed  $H_\infty$  tracking control for strict feedback nonlinear systems, *Nonlinear Anal. Model. Control*, **22**(3):317–333, 2017.
12. Z.Q. GAO, Scaling and bandwidth-parameterization based controller tuning, in *Proceedings of the 2003 American Control Conference, Denver, June 4–6, 2003*, IEEE, Piscataway, NJ, 2003, pp. 4989–4996.
13. N. Guenard, T. Hamel, R. Mahony, A practical visual servo control for an unmanned aerial vehicle, *IEEE Trans. Rob.*, **24**(2):331–340, 2008.
14. J.Q. Han, *Active disturbance rejection control technique: The technique for estimating and compensating the uncertainties*, National Defense Industry Press, Beijing, 2008 (in Chinese).
15. J.Q. Han, From PID to active disturbance rejection control, *IEEE Trans. Ind. Electron.*, **56**(3): 900–906, 2009.
16. V.R. Komma, P.K. Jain, N.K. Mehta, An approach for agent modeling in manufacturing on JADE (TM) reactive architecture, *Int. J. Adv. Manuf. Technol.*, **52**(9–12):1079–1090, 2011.
17. H. Liu, X.L. Hou, J. Kim, Y. Zhong, Decoupled robust velocity control for uncertain quadrotors, *Asian J. Control*, **17**(1):225–233, 2015.
18. D. Mellinger, N. Michael, V. Kumar, Trajectory generation and control for precise aggressive maneuvers with quadrotors, *The International Journal of Robotics Research*, **31**(5):664–674, 2012.
19. B.X. Mu, K.W. Zhang, Y. Shi, Integral sliding mode flight controller design for a quadrotor and application in a heterogeneous multi-agent system, *IEEE Trans. Ind. Electron.*, **64**(12):9389–9398, 2017.
20. G.V. Raffo, M.G. Ortega, F.R. Rubio, Robust nonlinear control for path tracking of a quad-rotor helicopter, *Asian J. Control*, **17**(1):142–156, 2015.
21. X.L. Shao, J. Liu, H.L. Wang, Robust back-stepping output feedback trajectory tracking for quadrotors via extended state observer and sigmoid tracking differentiator, *Mech. Syst. Signal Process.*, **104**(2018):631–647, 2018.
22. C.L. Tian, J.W. Wang, Z.J. Yin, G.H. Yu, Integral backstepping based nonlinear control for quadrotor, in *Proceedings of the 35th Chinese Control Conference, Chengdu, July 27–29, 2016*, CAA, Shanghai, 2016, pp. 10581–10585.
23. E.R. Valeria, R.E. Caldera, S.C. Lara, J. Guichard, LQR control for a quadrotor using unit quaternions: Modeling and simulation, in *Proceedings of International Conference on Electronics, Communications and Computing, Cholula, Puebla, Mexico, March 11–13, 2013*, IEEE, Piscataway, NJ, 2013, pp. 172–178.

24. C.L. Wang, Z.Q. Chen, Q.L. Sun, Q. Zhang, Design of pid and adrc based on quadrotor helicopter control system, in *Proceedings of the 2016 Chinese Control and Decision Conference, Yinchuan, May 28–30, 2016*, IEEE, Piscataway, NJ, 2016, pp. 5860–5865.
25. H.Q. Wang, X.P. Liu, S. Li, D. Wang, Adaptive neural output-feedback control for a class of non-lower triangular nonlinear systems with unmodeled dynamics, *IEEE Trans. Neural Networks Learn. Syst.*, **29**(8):3658–3668, 2018.
26. H.Q. Wang, X.P. Liu, B. Niu, Robust fuzzy adaptive tracking control for nonaffine stochastic nonlinear switching systems, *IEEE Trans. Cybern.*, **48**(8):2462–2471, 2018.
27. S. Zeghlache, D. Saigaa, K. Kara, A. Harrag, A. Bouguerra, Backstepping sliding mode controller improved with fuzzy logic: Application to the quadrotor helicopter, *Arch. Control Sci.*, **22**(3):315–342, 2012.
28. X. Zhang, B. Xian, B. Zhao, Y. Zhang, Automomous flight control of a nano quadrotor helicopter in a GPS-denied environment using on-board vision, *IEEE Trans. Ind. Electron.*, **62**(10):6392–6403, 2015.
29. Z.C. Zhang, Y.Q. Wu, Modeling and adaptive tracking for stochastic nonholonomic constrained mechanical systems, *Nonlinear Anal. Model. Control*, **21**(2):166–184, 2016.
30. X.D. Zhao, X.Y. Wang, G.D. Zong, H.M. Li, Fuzzy-approximation-based adaptive output-feedback control for uncertain non-smooth nonlinear systems, *IEEE Trans. Fuzzy Syst.*, **26**(6): 3847–3859, 2018.
31. Q. Zheng, L.L. Dong, H.L. Dae, Z.Q. Gao, Active disturbance rejection control for MEMS gyroscopes, *IEEE Trans. Control Syst. Technol.*, **17**(6):1432–1438, 2009.